IEEE Access
Multidisciplinary | Rapid Review | Open Access Journal

Received December 20, 2016, accepted February 9, 2017, date of publication February 20, 2017, date of current version March 15, 2017.

Digital Object Identifier 10.1109/ACCESS.2017.2672206

Electromagnetic Coupling and Tunneling Through Chiral Layers

FAROQ RAZZAZ AND MAJEED A. S. ALKANHAL
Department of Electrical Engineering, King Saud University, Riyadh 11421, Saudi Arabia
Corresponding author: M. A. S. Alkanhal (majeed@ksu.edu.sa)

This work was supported in part by the College of Engineering Research Center, and in part by the Deanship of Scientific Research at King Saud University, Riyadh, Saudi Arabia.

ABSTRACT This paper presents a theoretical investigation of electromagnetic wave coupling and tunneling through chiral-chiral interfaces. The dispersion relation, conditions of the trapped modes, and evanescent wave coupling and tunneling in an optically active chiral slab and chiral ambient medium are derived. The transfer matrix method is developed to obtain the transmission and reflection coefficients across the chiral slab. The formation of discrete trapped modes and the continuous interval, where the discrete trapped modes are embedded, are determined by the chirality parameter of the chiral slab. The instantaneous field components, revealed via evanescent wave coupling and tunneling through the chiral slab interfaces, are also reported.

INDEX TERMS Chiral interfaces, evanescent waves, wave coupling, wave tunneling.

I. INTRODUCTION

Recently, technologies based on electromagnetic and optical materials have made significant progress. Cutting-edge electromagnetic (EM) materials, where major developments are being made, include metamaterials and optically active chiral materials. In recent years, numerous studies have explored the interaction of electromagnetic waves with chiral media. The primary property of chiral media is optical activity because it can rotate the polarization of linearly polarized plane waves propagating through the media [1]. Another important property of chiral media is circular dichroism, which refers to the different absorption of right and left circularly polarized waves inside the chiral medium [2]. Additionally, electric and magnetic fields are cross-coupled in chiral media.

The propagation of EM waves through dielectric chiral interfaces and through infinite chiral slabs was studied in [3]. That research confirmed the rotation of polarization of incident waves inside chiral materials. Chirowaveguides and their unique properties were introduced in [4]. Due to the optically active material inside the waveguide, chirowaveguides cannot support transverse electric (TE), transverse magnetic (TM), or transverse electromagnetic (TEM) modes separately, but they manifest mode-bifurcation in hybrid forms [4]–[6]. Additionally, the dispersion relations and field distribution of the hybrid propagating modes in chiral slabs, placed in a homogeneous symmetrical isotropic medium, were presented in [7]. The reflection and transmission characteristics of chiral media were also investigated in several published works [8]–[11]. The constitutive relation parameters of chiral media can be retrieved using several techniques, such as the state-space approach [2] and the transfer matrix technique [12] from the transmission and reflection coefficients, or from the dispersion relation [13]. Scattering and shielding of EM waves from a chiral material have been extensively studied in the literature [14]–[23]. Scattering by intrinsic optically active cylinders, with approximate expressions for small cylinders as compared to the incident wavelength, were modeled in [14]. A simple integral equation and method of moment solution to the problem of TE and TM scattering from a lossy homogeneous chiral cylinder of arbitrary cross-section can be obtained by replacing the cylinder with equivalent electric- and magnetic-surface currents [15]. Scattering and shielding characteristics of chiral-coated fibers have been studied using the state-equation approach [21].

The present work studies the atypical electromagnetic transmission and evanescent wave behavior in chiral slabs, emphasizing the evanescent wave penetration by coupling and tunneling through chiral layers. Accordingly, formation of discrete trapped modes in the chiral slab is investigated. The transfer matrix method (TMM) is employed to derive the transmission and reflection coefficients across the chiral slab. Additionally, the instantaneous field components in the chiral ambient medium and the chiral slab are presented. The effects

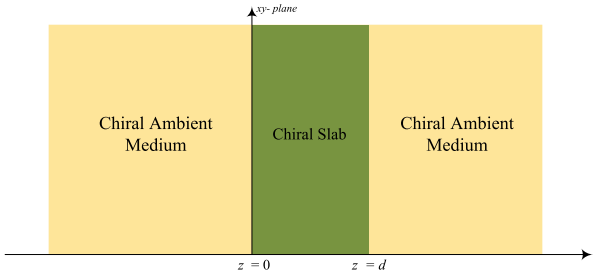

FIGURE 1. Geometry of the problem.

of the chirality parameter on the band where the discrete trapped modes are embedded, and the number of discrete trapped modes, are also explored. Further understanding of this EM behavior in optically active materials is expected to exert a notable influence on diagnosing and characterizing such materials, and therefore to have several implications in the design of forthcoming electromagnetic and optical devices.

II. FORMULATION AND ANALYSIS

To investigate the interaction of the evanescent and propagating EM waves through chiral interfaces, consider the physical model shown in Fig. 1, where a chiral slab is placed in a chiral ambient medium. Both chiral ambient media and the chiral slab support both propagating and evanescent modes at the same parallel wavevector. The following constitutive relations are used to characterize the chiral media:

$$\begin{aligned} \bar{D} &= \varepsilon \bar{E} - j\kappa \bar{H} \\ \bar{B} &= j\kappa \bar{E} + \mu \bar{H}, \end{aligned} \tag{1}$$

where ε, μ, and κ are the permittivity, permeability, and the chirality parameter of the medium, respectively.

Consider general obliquely incident plane waves with time dependency $e^{-i\omega t}$. The fields are defined as

$$\begin{aligned} \mathbf{E}(x, y, z; t) &= \mathbf{E_0} e^{i(k_x x + k_y y + k_z z - \omega t)} \\ &= \begin{bmatrix} E_x(z) \\ E_y(z) \\ E_z(z) \end{bmatrix} e^{i(k_x x + k_y y - \omega t)}, \end{aligned} \tag{2a}$$

and

$$\begin{aligned} \mathbf{H}(x, y, z; t) &= \mathbf{H_0} e^{i(k_x x + k_y y + k_z z - \omega t)} \\ &= \begin{bmatrix} H_x(z) \\ H_y(z) \\ H_z(z) \end{bmatrix} e^{i(k_x x + k_y y - \omega t)}, \end{aligned} \tag{2b}$$

where $K = (k_x, k_y)$ is the wavevector parallel to the chiral layer and ω is the angular frequency of the incident plane wave. Using the Berreman 4×4 matrix method [24], the Maxwell equations are reduced to four ordinary differential equations for the tangential components of the electric and magnetic fields:

$$\frac{d\Psi(z)}{dz} = iJA\Psi(z). \tag{3}$$

A. FIELDS IN THE CHIRAL AMBIENT MEDIUM

The chiral ambient medium has the following general properties: ε_a, μ_a, and κ_a. These properties are selected to provide two real and two imaginary z-directional wavenumbers, corresponding to propagating and evanescent modes, respectively. These modes are the eigenvalues of the 4×4 matrix iJA in the medium:

$$k_{zR}^{ae} = \pm\sqrt{\frac{\omega^2}{c^2}(\varepsilon_a\mu_a + \kappa_a)^2 - k_x^2}, \tag{4}$$

and

$$k_{zL}^{ap} = \pm\sqrt{\frac{\omega^2}{c^2}(\varepsilon_a\mu_a - \kappa_a)^2 - k_x^2}, \tag{5}$$

where the superscripts ap and ae refer to propagating and evanescent modes in the ambient medium, respectively. The corresponding tangential field components (eigenvectors) associated with these wavenumbers are given by

$$v_{\pm R}^{ae} = \begin{bmatrix} \pm k_{zR}^{ae} \dfrac{\left(\varepsilon_a\mu_a - \kappa_a\sqrt{\varepsilon_a\mu_a}\right)}{\frac{\omega}{c}\varepsilon_a\left(\varepsilon_a\mu_a - \kappa_a^2\right)} \\ i\sqrt{\dfrac{\mu_a}{\varepsilon_a}} \\ \dfrac{\mp ik_{zR}^{ae}}{\frac{\omega}{c}\left(\sqrt{\varepsilon_a\mu_a} + \kappa_a\right)} \\ 1 \end{bmatrix}, \tag{6}$$

and

$$v_{\pm L}^{ap} = \begin{bmatrix} \pm k_{zL}^{ap} \dfrac{\left(\varepsilon_a\mu_a + \kappa_a\sqrt{\varepsilon_a\mu_a}\right)}{\frac{\omega}{c}\varepsilon_a\left(\varepsilon_a\mu_a - \kappa_a^2\right)} \\ -i\sqrt{\dfrac{\mu_a}{\varepsilon_a}} \\ \dfrac{\pm ik_{zL}^{ap}}{\frac{\omega}{c}\left(\sqrt{\varepsilon_a\mu_a} - \kappa_a\right)} \\ 1 \end{bmatrix}. \tag{7}$$

The R and L refer to the right circularly polarized (RCP) and left circularly polarized (LCP) waves in the chiral medium, respectively.

In this exploration, the propagating LCP wavenumber $\left(k_{zL}^{ap}\right)$ is real, while the evanescent RCP wavenumber $\left(k_{zR}^{ae}\right)$ should be imaginary. Therefore, for the chiral ambient medium to support these two modes instantaneously, the parameters of the medium must satisfy the following conditions:

$$(\varepsilon_a\mu_a - \kappa_a)^2 > \frac{k_x^2}{\left(\frac{\omega}{c}\right)^2}, \quad (\varepsilon_a\mu_a + \kappa_a)^2 < \frac{k_x^2}{\left(\frac{\omega}{c}\right)^2}, \tag{8}$$

which implies that $\kappa_a < 0$.

B. FIELDS IN THE CHIRAL SLAB MEDIUM

The chiral slab has the following general properties: ε_s, μ_s, and κ_s. These properties are, also, selected to provide two real and two imaginary z-directional wavenumbers, corresponding to propagating and evanescent modes, respectively.

These modes are the eigenvalues of the 4×4 matrix iJA in the medium:

$$k_{zR}^{se} = \pm\sqrt{\frac{\omega^2}{c^2}\left(\varepsilon_s\mu_s + \kappa_s\right)^2 - k_x^2}, \tag{9}$$

and

$$k_{zL}^{sp} = \pm\sqrt{\frac{\omega^2}{c^2}\left(\varepsilon_s\mu_s - \kappa_s\right)^2 - k_x^2}, \tag{10}$$

where the superscripts sp and se refer to propagating and evanescent modes in the chiral slab medium, respectively. The corresponding tangential field components (eigenvectors) associated with these wavenumbers are given by

$$v_{\pm R}^{se} = \begin{bmatrix} \pm k_{zR}^{se}\dfrac{\left(\varepsilon_s\mu_s + \kappa_s\sqrt{\varepsilon_s\mu_s}\right)}{\frac{\omega}{c}\varepsilon_s\left(\varepsilon_s\mu_s - \kappa_s^2\right)} \\ i\sqrt{\dfrac{\mu_s}{\varepsilon_s}} \\ \dfrac{\mp ik_{zR}^{se}}{\frac{\omega}{c}\left(\sqrt{\varepsilon_s\mu_s} + \kappa_s\right)} \\ 1 \end{bmatrix}, \tag{11}$$

and

$$v_{\pm L}^{sp} = \begin{bmatrix} \pm k_{zL}^{sp}\dfrac{\left(\varepsilon_s\mu_s - \kappa_s\sqrt{\varepsilon_s\mu_s}\right)}{\frac{\omega}{c}\varepsilon_s\left(\varepsilon_s\mu_s - \kappa_s^2\right)} \\ -i\sqrt{\dfrac{\mu_s}{\varepsilon_s}} \\ \dfrac{\pm ik_{zL}^{sp}}{\frac{\omega}{c}\left(\sqrt{\varepsilon_s\mu_s} - \kappa_s\right)} \\ 1 \end{bmatrix}. \tag{12}$$

In this exploration, the propagating RCP wavenumber $\left(k_{zR}^{sp}\right)$ is real while the evanescent LCP wavenumber $\left(k_{zL}^{ae}\right)$ should be imaginary. Therefore, for the chiral slab medium that supports these two modes instantaneously, the parameters of the medium must satisfy the following conditions:

$$\left(\varepsilon_s\mu_s + \kappa_s\right)^2 > \frac{k_x^2}{\left(\frac{\omega}{c}\right)^2}, \quad \left(\varepsilon_s\mu_s - \kappa_s\right)^2 < \frac{k_x^2}{\left(\frac{\omega}{c}\right)^2}, \tag{13}$$

which implies that $\kappa_s > 0$.

Evanescent wave coupling at the chiral interface arises when the incident frequencies belong to the continuous spectrum interval I, and the RCP field components of the chiral ambient evanescent modes match those of the propagating modes in the chiral interface. Conversely, the propagating waves in the chiral ambient medium, with frequencies that belong to the band I, can be tunneled to the other side of the chiral slab by means of evanescent waves across the chiral slab. This phenomenon is similar to the tunneling of particles in quantum mechanics. Therefore, the construction of the trapped modes in the slab can be determined by matching the evanescent RCP fields in the ambient medium with the RCP propagating fields in the chiral slab at the interfaces.

The fields in the chiral ambient media ($z < 0$ and $z > d$) and in the chiral slab ($0 < z < d$) are given by

$$\begin{bmatrix} E_x \\ E_y \\ H_x \\ H_y \end{bmatrix} = C_1 \begin{bmatrix} -k_{zR}^{ae}\dfrac{\left(\varepsilon_a\mu_a - \kappa_a\sqrt{\varepsilon_a\mu_a}\right)}{\frac{\omega}{c}\varepsilon_a\left(\varepsilon_a\mu_a - \kappa_a^2\right)} \\ i\sqrt{\dfrac{\mu_a}{\varepsilon_a}} \\ ik_{zR}^{ae} \\ \dfrac{\frac{\omega}{c}\left(\sqrt{\varepsilon_a\mu_a} + \kappa_a\right)}{1} \end{bmatrix} e^{-ik_{zR}^{ae}z} \quad (z < 0),$$

$$= C_2 \begin{bmatrix} k_{zR}^{sp}\dfrac{\left(\varepsilon_s\mu_s - \kappa_s\sqrt{\varepsilon_s\mu_s}\right)}{\frac{\omega}{c}\varepsilon_s\left(\varepsilon_s\mu_s - \kappa_s^2\right)} \\ i\sqrt{\dfrac{\mu_s}{\varepsilon_s}} \\ -ik_{zR}^{sp} \\ \dfrac{\frac{\omega}{c}\left(\sqrt{\varepsilon_s\mu_s} + \kappa_s\right)}{1} \end{bmatrix} e^{ik_{zR}^{sp}z}$$

$$+ C_3 \begin{bmatrix} -k_{zR}^{sp}\dfrac{\left(\varepsilon_s\mu_s - \kappa_s\sqrt{\varepsilon_s\mu_s}\right)}{\frac{\omega}{c}\varepsilon_s\left(\varepsilon_s\mu_s - \kappa_s^2\right)} \\ i\sqrt{\dfrac{\mu_s}{\varepsilon_s}} \\ ik_{zR}^{sp} \\ \dfrac{\frac{\omega}{c}\left(\sqrt{\varepsilon_s\mu_s} + \kappa_s\right)}{1} \end{bmatrix} e^{-ik_{zR}^{sp}z} \quad (0 < z < d), \text{ and}$$

$$= C_4 \begin{bmatrix} k_{zR}^{ae}\dfrac{\left(\varepsilon_a\mu_a - \kappa_a\sqrt{\varepsilon_a\mu_a}\right)}{\frac{\omega}{c}\varepsilon_a\left(\varepsilon_a\mu_a - \kappa_a^2\right)} \\ i\sqrt{\dfrac{\mu_a}{\varepsilon_a}} \\ -ik_{zR}^{ae} \\ \dfrac{\frac{\omega}{c}\left(\sqrt{\varepsilon_a\mu_a} + \kappa_a\right)}{1} \end{bmatrix} e^{ik_{zR}^{ae}(z-d)} \quad (z > d), \tag{14}$$

where C_1, C_2, C_3, and C_4 are constants to be determined by applying the correct boundary conditions. Equation (14) presents the tangential field components inside and outside the chiral slab. These components are the evanescent fields in regions ($z < 0$ and $z > d$) and the propagation in region ($0 < z < d$). The continuity of the pertinent tangential field components at the interfaces ($z = 0, z = d$) yields

$$\begin{bmatrix} -k_{zR}^{ae}T_a & k_{zR}^{sp}T_s & -k_{zR}^{sp}T_s & 0 \\ 1 & -1 & -1 & 0 \\ 0 & -k_{zR}^{sp}T_s e^{-ik_{-}^{sp}d} & k_{zR}^{sp}T_s e^{ik_{-}^{sp}d} & -k_{zR}^{ae}T_a \\ 0 & e^{-ik_{-}^{sp}d} & e^{ik_{-}^{sp}d} & -1 \end{bmatrix} \begin{bmatrix} C_1 \\ C_2 \\ C_3 \\ C_4 \end{bmatrix} = 0. \tag{15}$$

For the above matrix to have a non-trivial solution, its determinant must be equal to zero; then, the trapped modes condition is given by

$$2\cos\left(k_{zR}^{sp}d\right) - i\left(\frac{k_{zR}^{ae}}{k_{zR}^{sp}}\frac{T_a}{T_s} + \frac{k_{zR}^{sp}}{k_{zR}^{ae}}\frac{T_s}{T_a}\right)\sin\left(k_{zR}^{sp}d\right) = 0, \tag{16}$$

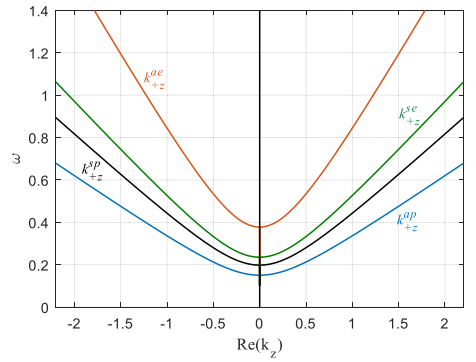

(a)

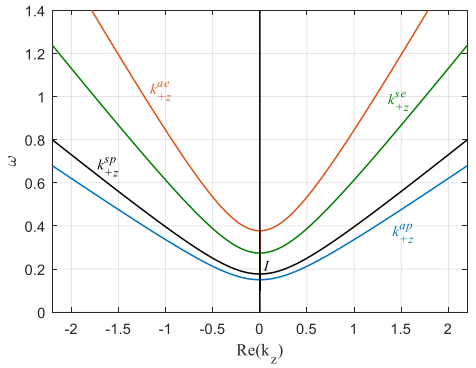

(b)

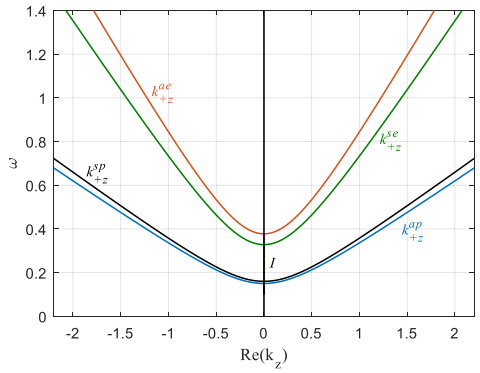

(c)

FIGURE 2. The dispersion relations (a) when $\kappa_s = 0.2$, (b) when $\kappa_s = 0.5$, and (c) when $\kappa_s = 0.8$. The blue and red lines are for the chiral ambient medium propagating and evanescent (RCL) z-directional wavenumber, respectively. The black and green lines are the propagating and evanescent (RCL) z-directional wavenumber of the chiral slab, respectively. The interval *I* is bounded by the (RCL) z-directional wavenumbers of the chiral slab.

where

$$T_a = \frac{\left(\varepsilon_a\mu_a - \kappa_a\sqrt{\varepsilon_a\mu_a}\right)}{\frac{\omega}{c}\varepsilon_a\left(\varepsilon_a\mu_a - \kappa_a^2\right)},$$

and

$$T_s = \frac{\left(\varepsilon_s\mu_s - \kappa_s\sqrt{\varepsilon_s\mu_s}\right)}{\frac{\omega}{c}\varepsilon_s\left(\varepsilon_s\mu_s - \kappa_s^2\right)}.$$

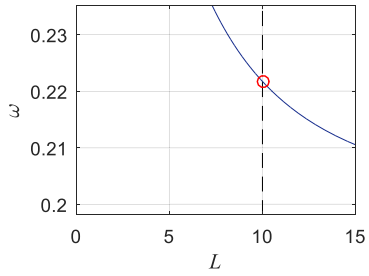

(a)

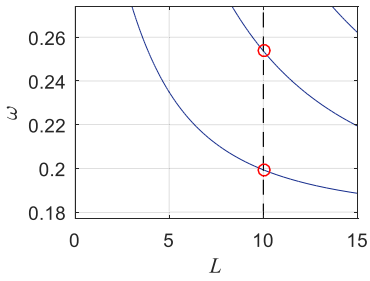

(b)

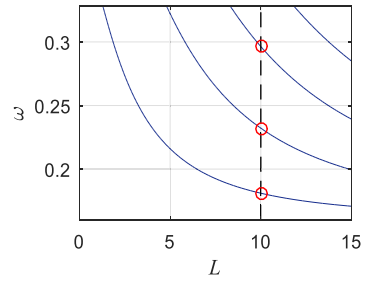

(c)

FIGURE 3. Trapped-mode frequencies as a function of the chiral slab thickness. (a) $\kappa_s = 0.2$, (b) $\kappa_s = 0.5$, and (c) $\kappa_s = 0.8$.

When an electromagnetic field is incident on the chiral slab, part of this field will be transmitted to the other side, and the other part of the field will be reflected. If the incident field hits the chiral slab at $z = 0$, the resulting field outside the slab will be as follows:

$$\psi(z) = \begin{cases} v_{+R}^{ap} e^{ik_{zR}^{ap} z} + r_{-R}^{p} v_{-R}^{ap} e^{-ik_{zR}^{ap} z} + r_{-R}^{e} v_{-R}^{ae} e^{-ik_{zR}^{ae} z} & (z < 0) \\ t_{+R}^{p} v_{+R}^{ap} e^{ik_{zR}^{ap}(z-d)} + t_{+R}^{e} v_{+R}^{ae} e^{ik_{zR}^{ae}(z-d)} & (z > d), \end{cases} \tag{17}$$

where $v_{+R}^{ap} e^{ik_{zR}^{ap} z}$ is the incident field, $v_{\pm R}^{ap,e}$ are the eigenvectors associated with the eigenvalues $\pm k_{zR}^{ap,e}$ in the anisotropic ambient medium, and $r_{-R}^{p,e}$ and $t_{+R}^{p,e}$ are the amplitudes of the reflected and transmitted fields, respectively.

The tangential field components at the interfaces of the chiral slab are continuous, so the field inside the slab can be found using the transfer matrix method [24] as

$$\psi(d) = T(0,d)\,\psi(0) \tag{18}$$

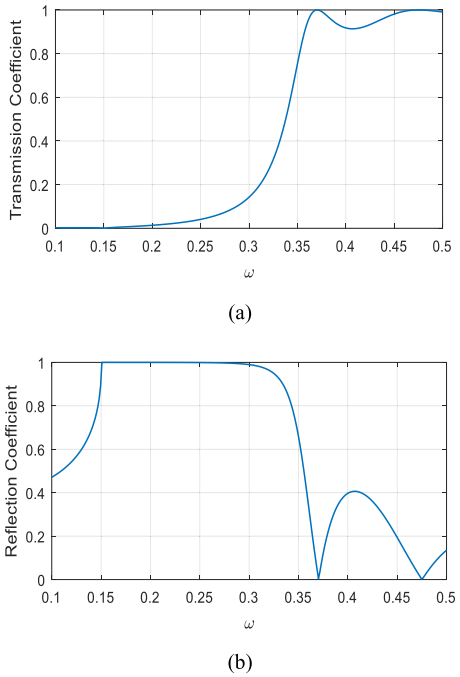

FIGURE 4. Transmission and reflection coefficients with $\kappa_s = 0.8$. (a) Transmission coefficient. (b) Reflection coefficient.

and

$$t^p_{+R}v^p_{+R} + t^e_{+R}v^e_{+R} = T\,(0,d)\left(v^p_{+R} + r^p_{-R}v^p_{-R} + r^e_{-R}v^e_{-R}\right), \tag{19}$$

where $T\,(0,d) = e^{iJA_s d}$ is the transfer matrix of the chiral layer. Then, the transmission and reflection coefficients can be determined directly from (19). For the case of ambient LCP evanescent wave coupling to the chiral slab, the materials should have $\kappa_a > 0$ and $\kappa_s < 0$. Hence, the trapped mode condition is also given by (16).

III. RESULTS AND DISCUSSION

To explore the behavior of the propagating and evanescent electromagnetic wave coupling, and tunneling through the chiral slab, the previously derived analytical formulations are used to examine the dispersion relations, trapped modes condition, and transmission coefficients in the chiral slab.

Consider the chiral ambient medium characterized by the following properties: $\varepsilon_a = 5.4$, $\mu_a = 1$, and $\kappa_a = -1$. The properties of the chiral slab are $\varepsilon_s = 5.4$, $\mu_s = 1$, with κ_s varied. The dispersion relations of the structure are shown in Fig. 2 for three chirality parameters, $\kappa_s = 0.3$, 0.5, and 0.8. As the chirality parameter increases, the continuous interval I, where the trapped modes are embedded, is widened. The interval I as a function of three different values of the chirality parameter is listed in Table 1.

Figure 3 shows the trapped modes embedded in the continuous interval I. As a result of expanding the continuous interval I, more possible trapped modes are included. For example, when the thickness of the chiral layer is set to 10 units ($d = 10$), there is only one perfect trapped mode when $\kappa_s = 0.2$. The frequency of this trapped mode is

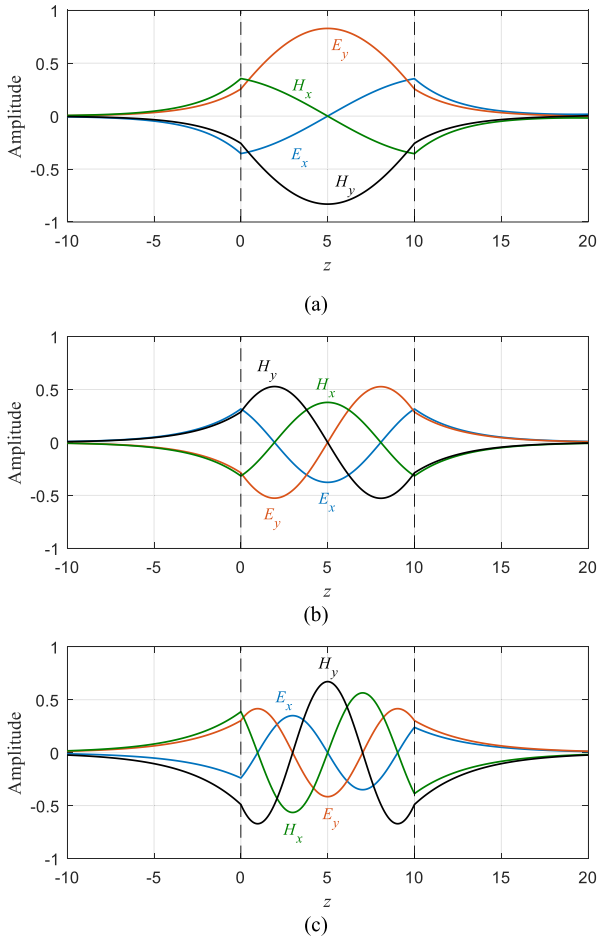

FIGURE 5. Instantaneous transverse fields at trapped mode frequencies. (a) $\kappa_s = 0.5$ and $\omega = 0.221721$, (b) $\kappa_s = 0.5$ and $\omega = 0.253719$, and (c) $\kappa_s = 0.8$ and $\omega = 0.296351$.

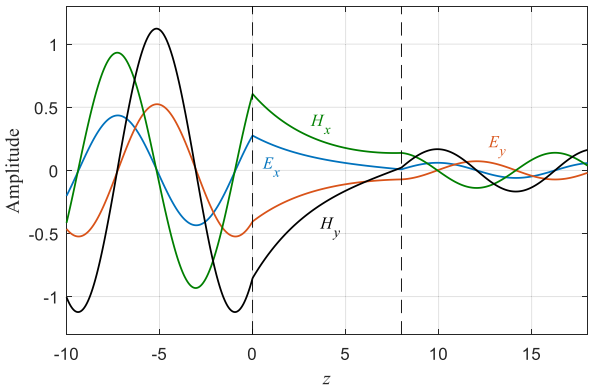

FIGURE 6. Tunneling of fields across the slab. $\kappa_s = 0.8$, $\omega = 0.27$, and $d = 8$.

$\omega = 0.221721$. However, for the same thickness of the chiral layer d $= 10$, there are two trapped modes when $\kappa_s = 0.5$; these trapped modes are located at $\omega = 0.199347$ and $\omega = 0.253719$. Additionally, there are three trapped modes when $\kappa_s = 0.8$, with frequencies $\omega = 0.181034$, $\omega = 0.232208$, and $\omega = 0.296351$.

The transmission and the reflection coefficients of the chiral slab, with $\kappa_s = 0.8$ as a function of the frequency,

TABLE 1. Interval I for different values of the chirality parameter.

κ_s	I
0.2	[0.198114, 0.235428]
0.5	[0.177066, 0.274154]
0.8	[0.160061, 0.328129]

are depicted in Fig. 4. The instantaneous field components at some trapped modes are depicted in Fig. 5. The instantaneous fields display the coupling between evanescent waves in the chiral ambient medium and the propagating fields in the chiral slab. For any frequency that belongs to the continuum frequency band I, propagating fields in the chiral ambient medium can be tunneled to the other side of the slab by means of the evanescent fields in the slab, as shown in Fig. 6.

IV. CONCLUSIONS

This paper presented a consolidated analytical investigation of the electromagnetic wave coupling and tunneling mechanisms through chiral layers. It focused on the characterization of the evanescent wave behavior and the physical conditions of the evanescent wave coupling and tunneling through chiral interfaces. Accordingly, the formation of discrete trapped modes in the chiral slab was investigated. The possible number and frequencies of these discrete trapped modes in the chiral slab were determined. The value of the chirality parameter has an evident effect on the trapped mode frequencies and on the width of the continuous interval where these discrete trapped modes are embedded. Electromagnetic evanescent wave tunneling through the chiral slab interfaces was confirmed if the incident wave frequencies belonged to the continuum interval of the embedded modes in the chiral slab. Lastly, the fields transmitted by the mechanisms of evanescent wave coupling and tunneling through chiral interfaces were evaluated using the Berreman matrix method.

REFERENCES

[1] P. Pelet and N. Engheta, "The theory of chirowaveguides," *IEEE Trans. Antennas Propag.*, vol. 38, no. 1, pp. 90–98, Jan. 1990.
[2] D. Zarifi, M. Soleimani, and A. Abdolali, "Parameter retrieval of chiral metamaterials based on the state-space approach," *Phys. Rev. E, Stat. Phys. Plasmas Fluids Relat. Interdiscip. Top.*, vol. 88, p. 023204, Aug. 2013.
[3] S. Bassiri, C. H. Papas, and N. Engheta, "Electromagnetic wave propagation through a dielectric–chiral interface and through a chiral slab," *J. Opt. Soc. Amer. A, Opt. Image Sci.*, vol. 5, pp. 1450–1459, Sep. 1988.
[4] N. Engheta and P. Pelet, "Modes in chirowaveguides," *Opt. Lett.*, vol. 14, pp. 593–595, Jun. 1989.
[5] S. F. Mahmoud, "Guided modes on open chirowaveguides," *IEEE Trans. Microw. Theory Techn.*, vol. 43, no. 1, pp. 205–209, Jan. 1995.
[6] S. F. Mahmoud, "On mode bifurcation in chirowaveguides with perfect electric walls," *J. Electromagn. Waves Appl.*, vol. 6, pp. 1381–1392, Jan. 1992.
[7] M. Oksanen, P. K. Koivisto, and I. V. Lindell, "Dispersion curves and fields for a chiral slab waveguide," *IEE Proc. H-Microw., Antennas Propag.*, vol. 138, no. 4, pp. 327–334, Aug. 1991.
[8] H. Cory and I. Rosenhouse, "Electromagnetic wave reflection and transmission at a chiral-dielectric interface," *J. Modern Opt.*, vol. 38, pp. 1229–1241, Jul. 1991.
[9] J. Lekner, "Optical properties of isotropic chiral media," *Pure Appl. Opt., J. Eur. Opt. Soc. A*, vol. 5, pp. 417–443, Jan. 1996.
[10] E. Georgieva, "Reflection and refraction at the surface of an isotropic chiral medium: Eigenvalue–eigenvector solution using a 4 × 4 matrix method," *J. Opt. Soc. Amer. A, Opt. Image Sci.*, vol. 12, pp. 2203–2211, Oct. 1995.
[11] A. Lakhtakia, V. V. Varadan, and V. K. Varadan, "A parametric study of microwave reflection characteristics of a planar achiral-chiral interface," *IEEE Trans. Electromagn. Compat.*, vol. 28, no. 2, pp. 90–95, May 1986.
[12] R. Zhao, T. Koschny, and C. M. Soukoulis, "Chiral metamaterials: Retrieval of the effective parameters with and without substrate," *Opt. Exp.*, vol. 18, pp. 14553–14567, Jul. 2010.
[13] C. Menzel, C. Rockstuhl, T. Paul, and F. Lederer, "Retrieving effective parameters for quasiplanar chiral metamaterials," *Appl. Phys. Lett.*, vol. 93, p. 233106, Dec. 2008.
[14] C. F. Bohren, "Scattering of electromagnetic waves by an optically active cylinder," *J. Colloid Interface Sci.*, vol. 66, pp. 105–109, Aug. 1978.
[15] M. A. Al-Kanhal and E. Arvas, "Electromagnetic scattering from a chiral cylinder of arbitrary cross section," *IEEE Trans. Antennas Propag.*, vol. 44, no. 7, pp. 1041–1048, Jul. 1996.
[16] R. D. Graglia, P. L. E. Uslenghi, and C. L. Yu, "Electromagnetic oblique scattering by a cylinder coated with chiral layers and anisotropic jump-immittance sheets," *J. Electromagn. Waves Appl.*, vol. 6, pp. 695–719, Jan. 1992.
[17] M. S. Kluskens and E. H. Newman, "Scattering by a chiral cylinder of arbitrary cross section," *IEEE Trans. Antennas Propag.*, vol. 38, no. 9, pp. 1448–1455, Sep. 1990.
[18] M. S. Kluskens and E. H. Newman, "Scattering by a multilayer chiral cylinder," *IEEE Trans. Antennas Propag.*, vol. 39, no. 1, pp. 91–96, Jan. 1991.
[19] Z. Chen, W. Hong, and W. Zhang, "Electromagnetic scattering from a chiral cylinder-general case," *IEEE Trans. Antennas Propag.*, vol. 44, no. 7, pp. 912–917, Jul. 1996.
[20] L. Kuzu, V. Demir, A. Z. Elsherbeni, and E. Arvas, "Electromagnetic scattering from arbitrarily shaped chiral objects using the finite difference frequency domain method," *Prog. Electromagn. Res.*, vol. 67, pp. 1–24, Jan. 2007.
[21] C.-N. Chiu and C. I. G. Hsu, "Scattering and shielding properties of a chiral-coated fiber-reinforced plastic composite cylinder," *IEEE Trans. Electromagn. Compat.*, vol. 47, no. 1, pp. 123–130, Feb. 2005.
[22] A. H. Sihvola and M. E. Ermutlu, "Shielding effect of hollow chiral sphere," *IEEE Trans. Electromagn. Compat.*, vol. 39, no. 3, pp. 219–224, Aug. 1997.
[23] J. A. Pereda, A. Grande, O. Gonzales, and A. Vegas, "FDTD modeling of chiral media by using the mobius transformation technique," *IEEE Antennas Wireless Propag. Lett.*, vol. 5, no. 1, pp. 327–330, Dec. 2006.
[24] D. W. Berreman, "Optics in stratified and anisotropic media: 4 × 4-matrix formulation," *J. Opt. Soc. Amer.*, vol. 62, pp. 502–510, Apr. 1972.

FAROQ RAZZAZ received the B.Sc. degree in communications engineering from Ibb University, Yemen, in 2007, and the M.Sc. degree in electrical engineering from King Saud University, where he is currently pursuing the Ph.D. and master's degrees with Electrical Engineering Department. He was a Teaching Assistant with Taiz University, Yemen.

MAJEED A. S. ALKANHAL received the Ph.D. degree in electrical engineering from Syracuse University, Syracuse, New York, in 1994. He is a Full Professor with the Department of Electrical Engineering, King Saud University, Riyadh, Saudi Arabia. He has served as a Consultant, Visiting Scholar, Editor, and Referee for several institutes and scientific journals. He has published books, book chapters, research papers, technical reports, and patents in his research fields. His research interests include wireless communications, radar systems, electromagnetic propagation and scattering in complex materials, microwave/millimeter-wave antenna design and optimization, modern optimization techniques, and computational electromagnetics.